INTERNATIONAL JOURNAL FOR NUMERICAL METHODS IN FLUIDS, VOL. 8, 151–164 (1988)

# IDENTIFICATION OF NON-DARCY GROUNDWATER FLOW PARAMETERS

I. M. GOODWILL AND C. KALLIONTZIS

*Department of Civil Engineering, University of Leeds, Leeds, LS2 9JT, U.K.*

## SUMMARY

Non-Darcy groundwater flow parameters are identified for three different flow systems. In the first system, which is essentially one-dimensional, the parameters are determined by means of an integral method. A rectangular parametric grid is used for the identification of the non-Darcy friction coefficients in the second system, which is two-dimensional. The parameters in the third system, which involves a hybrid simulation of three-dimensional flow, are optimized by adopting a constrained non-linear programming technique. This technique combines Cauchy's steepest-descent method together with the modeller's subjective judgement of the results at the end of each iterative step. The paper is concluded with a brief description of the additional research which is thought to be necessary before the difficulties of optimizing the non-Darcy flow parameters can be overcome.

KEY WORDS Non-Darcian flow Inverse problem Finite differences Finite elements

## INTRODUCTION

The accurate simulation of groundwater flow largely depends upon a set of coefficients which firstly characterize the internal structure of the porous medium and secondly reflect the properties of the fluid that moves through the granular matrix. The process of obtaining optimal values of these parameters is known as the inverse problem. In practice this amounts to determining optimal values for a number of aquifer parameters in order to achieve the minimization of a calibration criterion (or objective function) which is based on either the water levels or the flow differences between a mathematical model and the experimental or field data.

There exist various approaches which may be adopted to solve this groundwater flow optimization problem. These are the direct,[1] linear,[2,3] non-linear[4–12] and stochastic[13] programming techniques. The most widely adopted optimization method in groundwater flow modelling is the non-linear programming technique. The efficiency of various optimization methods has been compared by Yeh.[14] Recently, Neuman[15] combined non-linear programming techniques with the Kriging method, which is a statistical technique akin to stochastic programming. Delhomme[16] and Gambolati and Volpi[17] also adopted the Kriging method for the determination of aquifer parameters. In all these applications, Darcy's resistance equation was assumed to be valid. To the authors' knowledge, the only non-Darcy flow parameter identification has been performed by Edgell[18] and Peters.[19] Edgell used Gauss's least-squares method, whereas Peters adopted the random search method.

In this paper an attempt is made to identify the non-Darcy flow parameters pertinent to three different flow systems. The first and second systems are applied in two-dimensional steady non-Darcy flow situations, whereas third system is used for the simulation of unsteady three-

0271–2091/88/020151–14$07.00

*Received 10 June 1986*
*Revised 20 March 1987*

dimensional non-Darcy flow. An integral method, a rectangular parametric grid with a linear calibration function and a constrained non-linear programming technique are the optimization methods used respectively for each system.

## THE ONE-DIMENSIONAL STEADY FLOW SYSTEM

This system is concerned with the determination of the free surface elevation and the discharge through an earth dam having vertical faces and being composed of gravel. The appropriate variables and boundary conditions are illustrated in Figure 1. The combination of Forchheimer's friction equation with the Dupuit–Forchheimer assumptions yields an equation of the form

$$-\mathrm{d}h/\mathrm{d}x = au + bu^2, \tag{1}$$

where $h$ is the free surface height, $u$ is the 'average' or 'bulk' velocity of the fluid in the $x$ direction and $a$ and $b$ are the friction coefficients. Equation (1) together with the continuity equation

$$\mathrm{d}(uh)/\mathrm{d}x = 0 \tag{2}$$

enable the elevation of the free surface to be determined. The discharge $Q$ per unit width of the aquifer, which is defined as

$$Q = uh, \tag{3}$$

duly satisfies the continuity equation. In order to account for the presence of the surface of seepage, the following empirical equation is included in the analysis:

$$u_e = m(h_e - h_d)^n, \tag{4}$$

where $h_e$ and $h_d$ are the water levels as defined in Figure 1, $u_e$ is the horizontal velocity within the

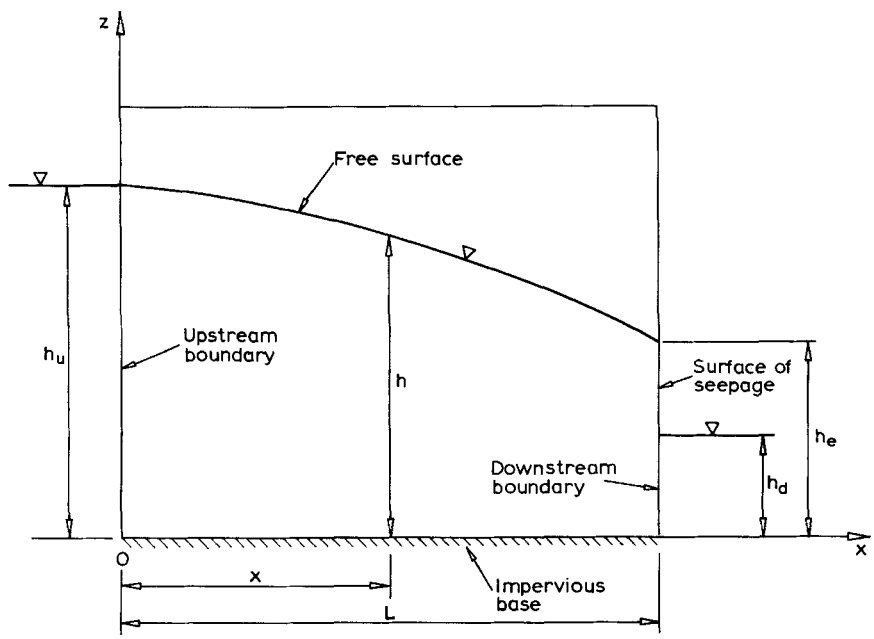


Figure 1. Boundary conditions and variable definition using a vertical cross-section of unconfined aquifer

aquifer at the downstream boundary and $m$ and $n$ are the surface of seepage equation parameters. Euler's finite difference method[20,21] was used for the solution of the system which comprises equations (1), (2) and (4). Prior to its application, the parameters $a$, $b$, $m$ and $n$ were identified by examining a number of experimental free surface profiles and discharges. Gauss's least-squares method yielded the surface of seepage equation coefficients, the values of which are given in Figure 2.

Edgell[18] and Peters[19] used a similar experimental procedure in order to evaluate the friction parameters $a$ and $b$. Edgell performed a least-squares analysis using equation (1), whereas Peters adopted a trial-and-error (or random search) method. Both approaches were based on a knowledge of the free surface slope defined by the term $-\mathrm{d}h/\mathrm{d}x$. Such methods, however, are error prone, since they can magnify even the slightest error in the water level data. When analysing a number of free surface curves, these techniques yield a unique set of $a$ and $b$ values for each curve. Therefore, to select representative $a$ and $b$ values, it is necessary either to average the coefficients obtained from each test or to adopt the ones that reappear consistently.

It was the above consideration that led to the selection of an integral method for the determination of the coefficients. Integration of equation (1) between the limits $x = 0$ and $x = L$, where $L$ is the length of the unconfined aquifer (Figure 1), yields

$$h_u - h_e = a \int_0^L u \, \mathrm{d}x + b \int_0^L u^2 \, \mathrm{d}x. \tag{5}$$

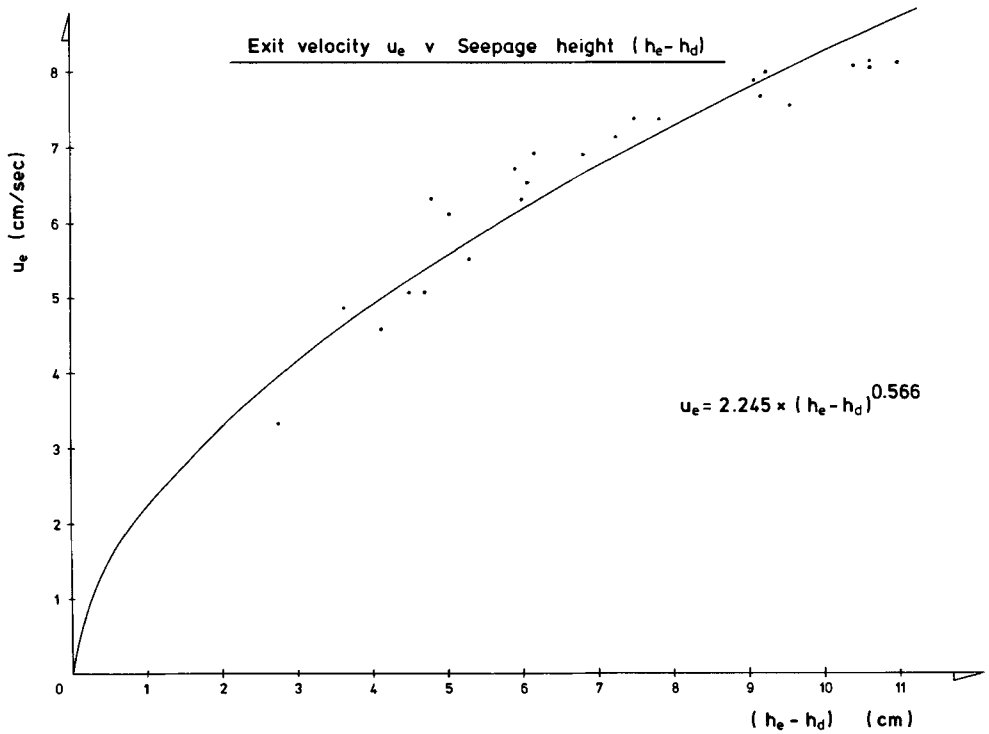


Figure 2. The correlation between the exit velocity ($u_e$) and the seepage height ($h_e - h_d$) at the downstream boundary

By rearranging equation (5) as

$$\frac{h_u - h_e}{\int_0^L u\,dx} = a + b\frac{\int_0^L u^2\,dx.}{\int_0^L u\,dx}, \tag{6}$$

it can be seen that the equation is linear and of the form

$$Y = a + bX, \tag{7}$$

where $Y$ and $X$ are experimentally known quantities. The parameters $a$ and $b$ are subsequently determined by applying Gauss's least-squares method to equation (7). Simpson's rule is used for the evaluation of the integrals. The experimental results together with the fitted line and the numerical values of the friction coefficients are presented in Figure 3. One of the advantages of this technique is that each experimental curve, though not appearing explicitly in equation (6), is incorporated into the integrals and therefore every point in Figure 3 corresponds to one set of experimental data. It follows that the parameters thus obtained are representative of the complete set of experimental results.

To establish the validity of the numerical values of the coefficients $a$, $b$, $m$ and $n$, equations (1), (2) and (4) were applied to the solution of the non-Darcy unconfined aquifer problem shown in Figure 1, using different boundary conditions. In all cases the numerical solutions compared very well with the experimental ones. A typically example is presented in Figure 4, where curve I is the experimentally determined free surface profile, curve II is the numerically computed free surface profile and curve III is the Dupuit parabola.

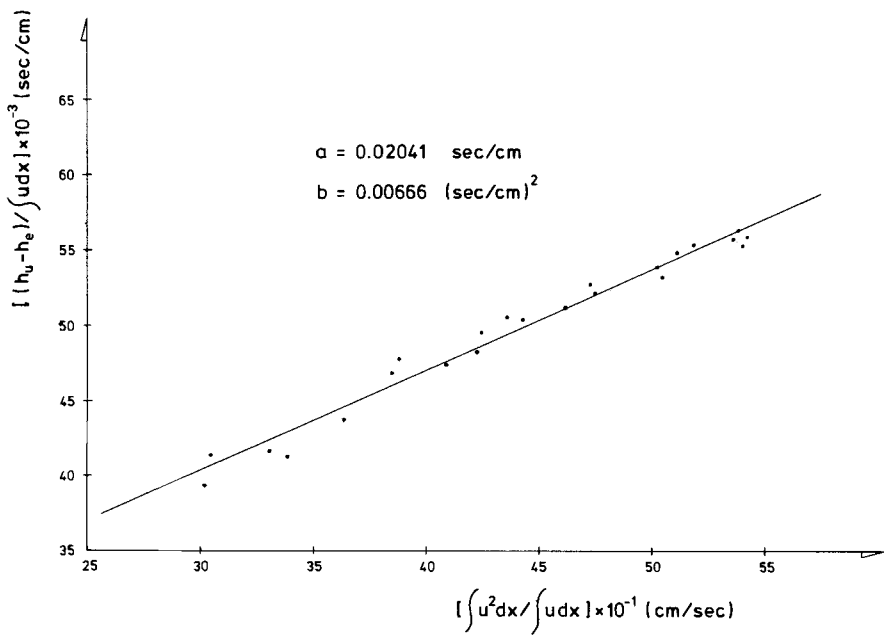


Figure 3. The correlation of the variables of equation (6) for the identification of the parameters $a$ and $b$

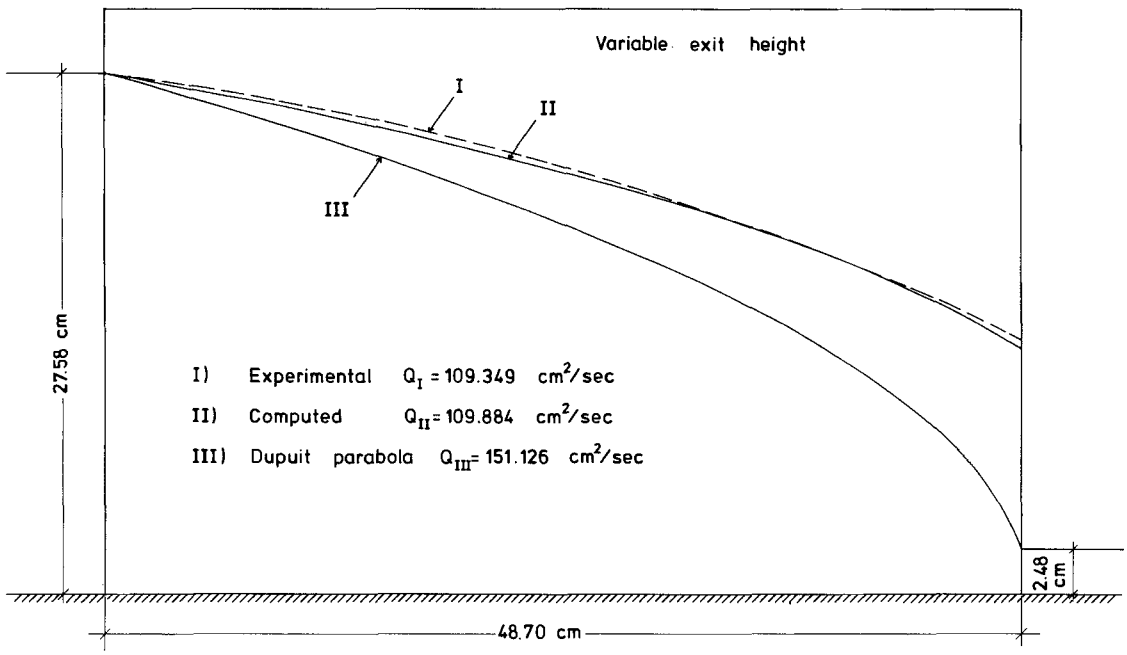


Figure 4. Comparison between numerical and experimental results for system I

## THE TWO-DIMENSIONAL STEADY FLOW SYSTEM

The second system is used for the simulation of the same non-Darcy unconfined aquifer situation as the previous one. In this case, however, the governing equation is two-dimensional and has the form

$$\frac{\partial}{\partial x}\left(K\frac{\partial \phi}{\partial x}\right)+\frac{\partial}{\partial z}\left(K\frac{\partial \phi}{\partial z}\right)=0, \tag{8}$$

where $\phi$ is the total head of the fluid and is defined as

$$\phi = p/\rho g + z, \tag{9}$$

where $p$ and $\rho$ are the pore pressure and density of the fluid respectively and $g$ is the gravitational constant. Also in equation (8) $K$ is the hydraulic conductivity, which for non-Darcy flow may be expressed as[22]

$$K=\frac{a}{2bI}\left[-1+\sqrt{\left(1+\frac{4bI}{a^2}\right)}\right], \tag{10}$$

where $a$ and $b$ are the Forchheimer friction parameters and $I$ is the hydraulic gradient given by

$$I=\left[\left(\frac{\partial \phi}{\partial x}\right)^2+\left(\frac{\partial \phi}{\partial z}\right)^2\right]^{0.5}. \tag{11}$$

The configuration of the flow domain and the relevant boundary conditions are presented in Figure 5. The solution of equation (8), subject to the boundary conditions of Figure 5, is achieved by means of triangular finite elements.[20]

Although the usual way of establishing the numerical values of $a$ and $b$ is the permeameter test, in

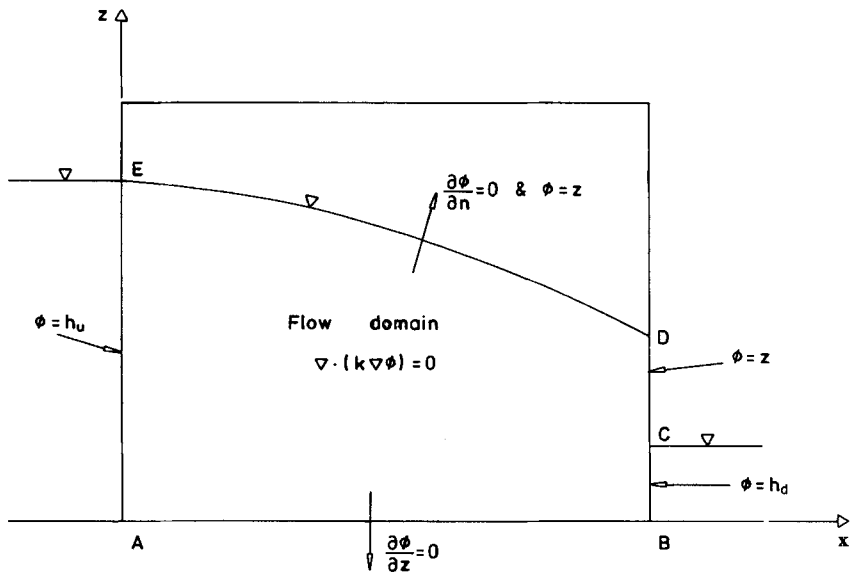


Figure 5. The flow domain and boundary conditions relative to system II

this paper the actual discharge and free surface profile data are used for their determination. Initially, the Gauss–Newton[23] method (or Marquardt's method as it is otherwise known) was incorporated into the finite element model. Although this method successfully minimized the water level error on which the objective function was based, however, it maximized the flow per unit width error. The reason for this performance lay firstly with the extra resistance to the flow which was offered by the permeable partitions (Figure 6), which held the gravel bank in a vertical position, and secondly with the small overall dimensions of the earth dam model (Figure 6). The outcome was a higher free surface elevation than would have otherwise occurred. The dimensions of the aquifer model were purposely designed to be modest, since the intention was to estimate the friction coefficients without the use of a permeameter, which for the case of gravel offers the well known difficulties of long length, large diameter and wall effect. It may be remarked that the first system, which was applied to the solution of the same flow problem as Figure 6, was able to account very well for the effect of the partitions on the flow phenomenon.

Subsequently, the optimization of an objective function, $J_c$, based on the flow per unit width prediction was adopted, since it was considered that the accurate determination of flow was more important than the determination of water levels. Hence

$$J_c = |Q_e - Q_c|, \tag{12}$$

where $Q_e$ is the experimental and $Q_c$ the computed discharge. Various techniques exist for the minimization of (12), some of which depend on the calibration function gradients which direct the solution towards the optimum point (i.e., where $J_c$ is a minimum), whereas others depend on function evaluations coupled with specific search patterns. The latter type is used in the present study.

From the published[24] Forchheimer friction coefficients, the following parametric constraints were chosen:

$$0{\cdot}007 \leqslant a \leqslant 0{\cdot}019\,\mathrm{s\,cm^{-1}}, \tag{13}$$

$$0{\cdot}007 \leqslant b \leqslant 0{\cdot}019\,\mathrm{s^2\,cm^{-2}}. \tag{14}$$

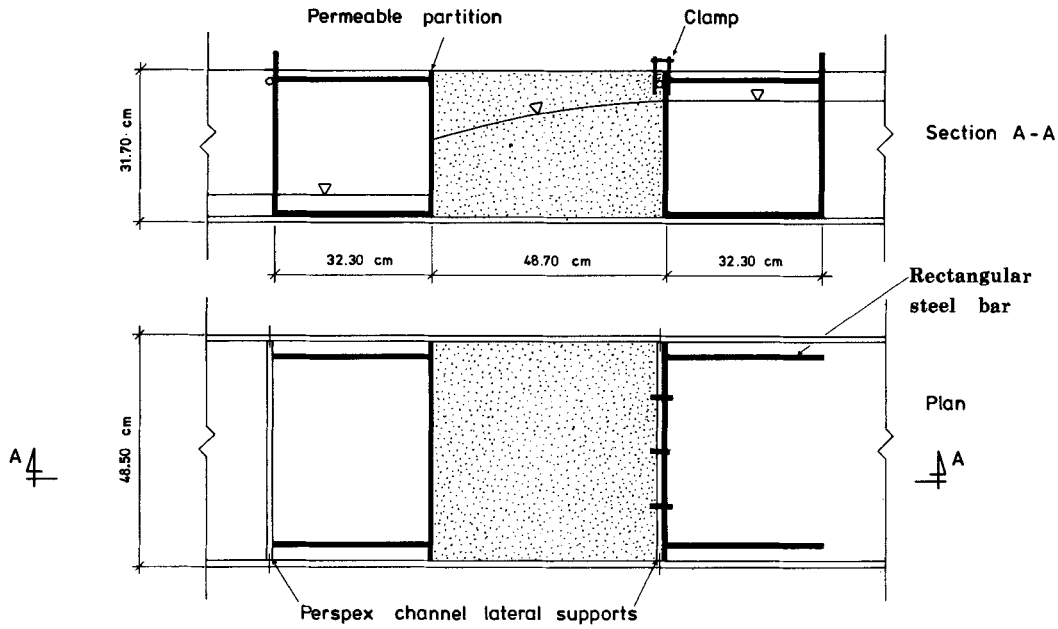


Figure 6. The experimental aquifer model analysed by systems I and II

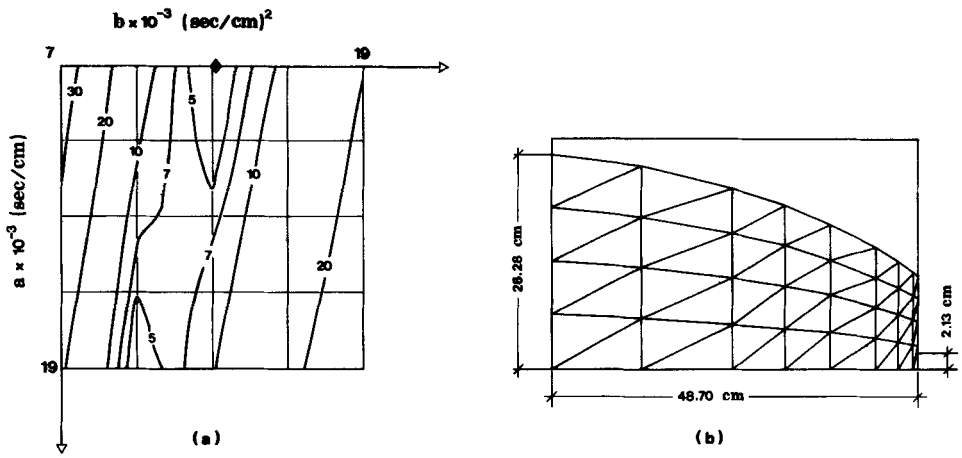


Figure 7. The parametric grid and the aquifer discretization in the case of system II: $^5$ calibration function contours; ◆ minimum $J_c$ location; $a_{opt} = 0{\cdot}00700$ s/cm; $b_{opt} = 0{\cdot}01308$ s$^2$/cm$^2$; min $J_c = 1{\cdot}834$ cm$^2$/s; $J_c = |Q_c - Q_c|$

As shown in Figure 7(*a*), the constrained area is divided into a rectangular grid system and at every node the calibration function is computed. In the finite element discretization of the flow domain, the experimental free surface is used as the upper boundary (Figure 7(*b*)). Thus the problem is reduced to one whereby only the flow per unit width is calculated using different coefficients. Having identified the node where $J_c$ is least, the optimum solution is then obtained by interpolating quadratically in one parametric direction at a time. If the minimum $J_c$ is found at the constraining boundaries, then only one parameter is optimized.

The same analysis was applied to the complete set of experimental data. The friction coefficients

thus obtained are presented in Figure 8, where $\bar{a}_{opt}$ and $\bar{b}_{opt}$ denote the finally selected coefficients (mean values of $a$ and $b$). Although parameter $b$ showed little variation from the mean, parameter $a$ varied quite strongly: in three cases the limiting value of 0·019 s cm$^{-1}$ was obtained, whereas at the other extreme the limiting value of 0·007 s cm$^{-1}$ frequently appeared as a solution. As expected, the mean parameters, when used for the solution of the complete flow problem, yielded very good discharge predictions and caused relatively poor free surface profiles to be produced in comparison with the experimental ones.

## THE THREE-DIMENSIONAL UNSTEADY FLOW SYSTEM

The third system is used for the simulation of unsteady three-dimensional non-Darcy groundwater flow. The plan of the unconfined aquifer that was investigated together with the location of the observation wells (or depth gauges) D1–D7 are presented in Figure 9. The equations for this system form part of a hybrid numerical model[20,21] which analyses three-dimensional groundwater flow by de-coupling it into a series of one-dimensional problems for the determination of the surface of seepage height at the downstream boundary and a two-dimensional problem for the determination of the free surface elevation within the flow domain. The boundary conditions for this flow problem (Figure 9) are:

(1) Upstream boundary ABC ($h_u = h_u(t)$).
(2) Downstream boundary GFED ($h_d = h_d(t)$), where the surface of seepage is formed.
(3) Impermeable boundary AG ($\partial h/\partial n = 0$).
(4) Impermeable boundary CD ($\partial h/\partial n = 0$).

Linear isoparametric finite elements are used for the discretization of the unconfined aquifer (Figure 10). The following are the equations adopted for the determination of the surface of seepage at GFED:[20,21]

$$\frac{d^2h}{dx^2} = \frac{u(a + 2bu)}{h}\frac{dh}{dx} \tag{15}$$

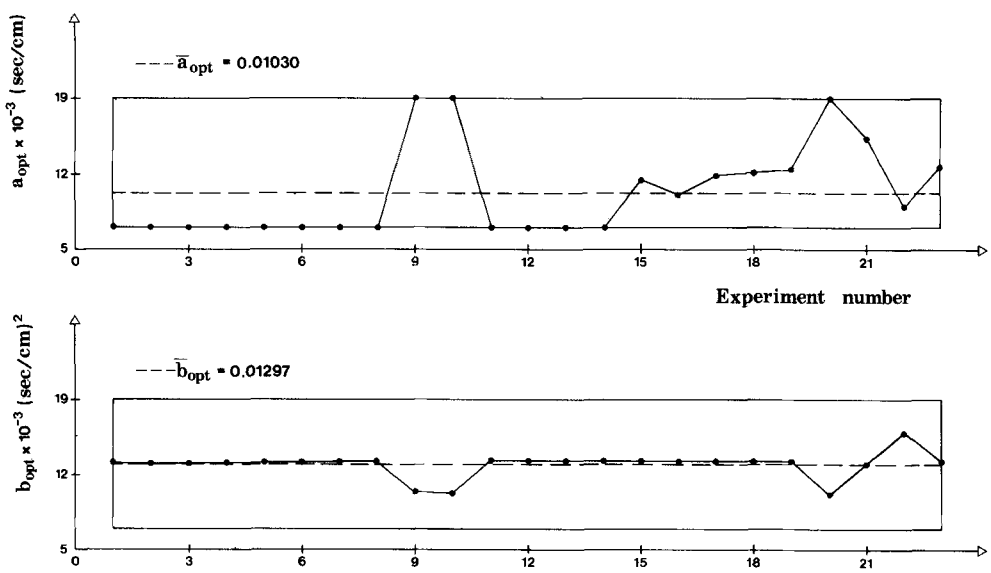


Figure 8. The friction coefficients identified using the complete set of experimental data

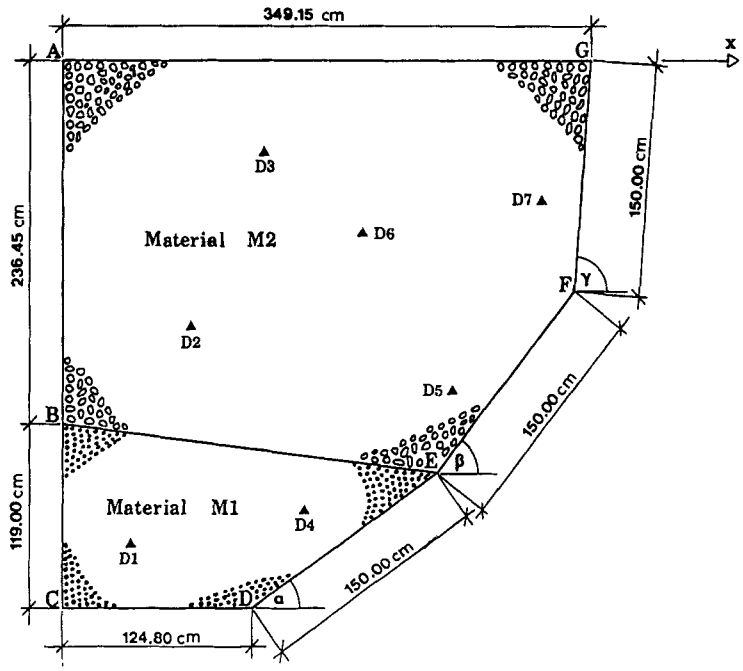


Figure 9. Plan of the unconfined aquifer analysed by system III; ▲, observation well location

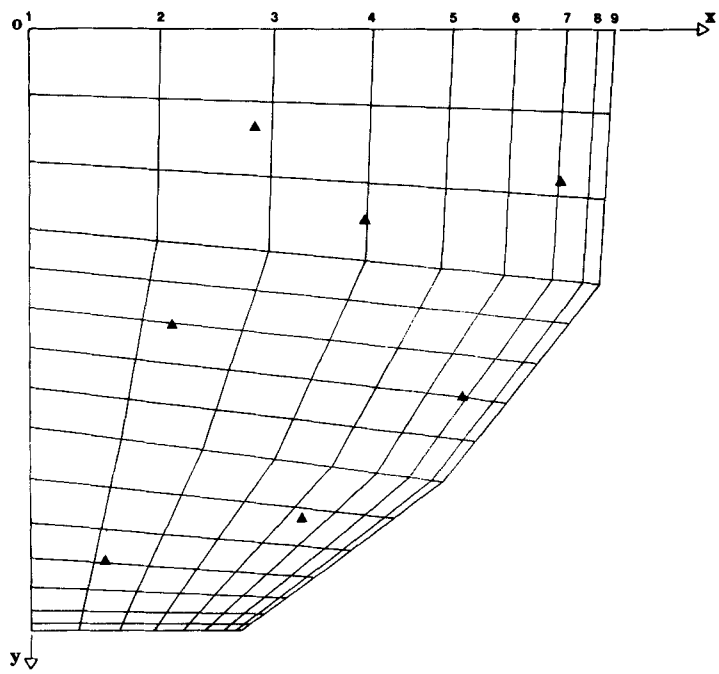


Figure 10. Discretization of the aquifer using linear isoparametric finite elements; ▲, observation well location

and

$$u_e = m(h_e - h_d)^n, \tag{16}$$

which are the same as those of the first flow system. Equations (15) and (16) are applied along the 'horizontal' lines which connect the upstream and the downstream boundaries. Euler's finite difference method was used for the solution of (15) and (16). Having calculated the height of the surface of seepage, the free surface elevation within the porous medium is then obtained from the continuity equation

$$\varepsilon \frac{\partial h}{\partial t} = \frac{\partial}{\partial x}\left(T\frac{\partial h}{\partial x}\right) + \frac{\partial}{\partial y}\left(T\frac{\partial h}{\partial y}\right), \tag{17}$$

where $\varepsilon$ is the volumetric or absolute porosity of the porous medium and $T$ is the transmissivity given by

$$T = \frac{ah}{2b}\left[-1 + \sqrt{\left(1 + \frac{4b}{a^2}\frac{\partial h}{\partial s}\right)}\right]\left(\frac{\partial h}{\partial s}\right)^{-1}, \tag{18}$$

where $a$ and $b$ are the non-Darcy friction parameters and $\partial h/\partial s$ is the hydraulic gradient, which may be expressed as

$$\frac{\partial h}{\partial s} = \left[\left(\frac{\partial h}{\partial x}\right)^2 + \left(\frac{\partial h}{\partial y}\right)^2\right]^{0.5}. \tag{19}$$

Equation (17) is solved by means of the finite element numerical technique. Further details of the model can be found elsewhere.[20,21]

The parameters $a, b, m, n$ and $\varepsilon$ which occur in equations (15)–(18) were next optimized. Relatively accurate initial estimates of the coefficients were previously obtained from a small-scale two-dimensional experimental model. The algorithm that is developed involves a search for the minimum of a calibration (or objective) function $C_f$ defined as

$$C_f = \sum_{t=2}^{t=\bar{T}} \sum_{d=1}^{d=7} \left(h_{exp} - h_{comp}\right)_{d,t}^2 \tag{20}$$

along directions of steepest descent. Thus the method may be classified as a non-linear programming technique. In equation (20) $\bar{T}$ is the total simulation period, $h_{exp}$ and $h_{comp}$ are the experimental and computed water levels and $d$ is a depth gauge index. The range of the parametric solutions was limited by imposing suitable constraints.

Initially, it was found that the minimization algorithm was very sensitive to the order in which the parameters were optimized. The alteration of the surface of seepage equation (equation (16)) coefficients yielded significant changes in the objective function $C_f$. The converse resulted when the friction coefficients or the porosity values were optimized first. In the latter case, the parametric values, which acted as constraints, frequently appeared as the optimum solution. Also minimization was difficult to achieve when the appropriate parameters were optimized separately for each material (shown as M1 and M2 in Figure 9).

Hence, as a first step, it was decided to optimize all the parameters simultaneously by using the formula

$$PM_i^{new} = (1 + S \times sign_i) \times PM_i^{old}, \tag{21}$$

where $PM_i$ denotes a parameter (Table I), $i$ is the parameter index ($i = 1$–$10$), $S$ is a constant assumed to be the same for all parameters and $sign_i$ is the search direction and is given by

Table I

| Parameter index $i$ ($PM_i$) | Symbol |
|---|---|
| 1 | $a_1$ (s cm$^{-1}$) |
| 2 | $b_1$ (s$^2$ cm$^{-2}$) |
| 3 | $a_2$ (s cm$^{-1}$) |
| 4 | $b_2$ (s$^2$ cm$^{-2}$) |
| 5 | $m_1$ (cm$^{1-n_1}$ s$^{-1}$) |
| 6 | $n_1$ (dimensionless) |
| 7 | $m_2$ (cm$^{1-n_2}$ s$^{-1}$) |
| 8 | $n_2$ (dimensionless) |
| 9 | $\varepsilon_1$ (dimensionless) |
| 10 | $\varepsilon_2$ (dimensionless) |

$$\text{sign}_i = -\left(\frac{C_f^{\text{new}} - C_f^{\text{old}}}{|C_f^{\text{new}} - C_f^{\text{old}}|}\right)_i . \tag{22}$$

It was found that for all the parameters $\text{sign}_i$ was positive. Therefore equation (21) becomes

$$PM_i^{\text{new}} = (1 + S)PM_i^{\text{old}}. \tag{23}$$

By varying $S$ from 0 to 1 (Figure 11(*a*)), an optimum value of $S = 0{\cdot}34$ was obtained. In Figure 11(*a*) this optimization step is referred to as iteration 1 and Table II shows the results of this step. (The subscripts of the symbols in Table I indicate the material number: 1 for M1 and 2 for M2.) Before proceeding to the second iteration, parametric constraints were imposed. The friction coefficients $a$ and $b$ were restrained as follows:

$$0{\cdot}007 \leqslant a \leqslant 0{\cdot}030 \text{ s cm}^{-1}, \tag{24}$$

$$0{\cdot}007 \leqslant b \leqslant 0{\cdot}030 \text{ s}^2 \text{ cm}^{-2}. \tag{25}$$

Using data from a small-scale earth dam constructed in the laboratory, the following limitations were imposed on $m$:

$$1{\cdot}50 \leqslant m \leqslant 7{\cdot}50. \tag{26}$$

At the completion of the first iteration, the values obtained for parameters 6, 8, 9 and 10 were all higher than experimental evidence suggested was possible. For this reason they were fixed at the values given in Table III. Thus the parameters used for iteration 2 are presented in Table III. In the 'Remarks' column of Table III the word 'variable' indicates that a parameter can be optimized, whereas the word 'fixed' indicates that a parameter remains unchanged during the optimization process.

In iteration 3, parameters 5 and 7 were optimized simultaneously, since they control the free surface elevation at the downstream boundary, while the other parameters were held constant. The value of $\text{sign}_i$ (equation (22)) was first determined and then a new coefficient $S$ which minimized $C_f$ was evaluated. In iterations 4 and 5 a similar procedure was followed for parameters 1 and 3 and 2 and 4 respectively. The final values are presented in Table IV and the calibration function minimization sequence is shown in Figure 11(*b*). The shape of the response surface was not investigated in detail, but at no time during the optimization procedure was there any indication that local minima had been found within the region defined by the parameter constraints.

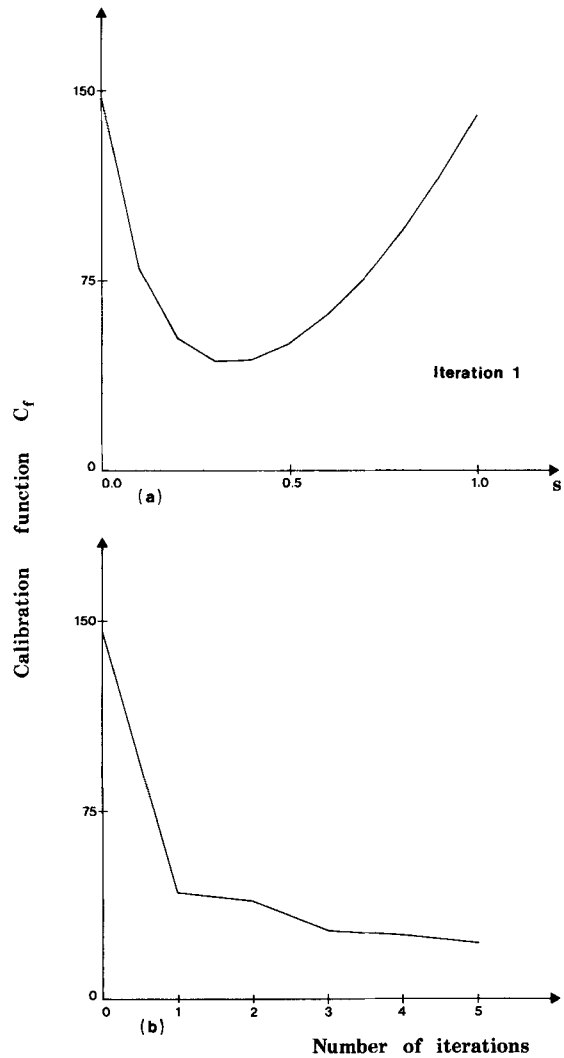


Figure 11. Calibration function minimization (*a*) during the first iteration and (*b*) for the total number of iterations

Table II

| Parameter number | Parameter values Before calibration $S = 0{\cdot}0$ | After calibration $S = 0{\cdot}34$ |
|---|---|---|
| 1 | 0·01569 | 0·02102 |
| 2 | 0·00905 | 0·01213 |
| 3 | 0·02041 | 0·02735 |
| 4 | 0·00666 | 0·00892 |
| 5 | 2·40500 | 3·22270 |
| 6 | 0·62100 | 0·83214 |
| 7 | 2·24500 | 3·00830 |
| 8 | 0·56600 | 0·75844 |
| 9 | 0·45700 | 0·61238 |
| 10 | 0·45100 | 0·60434 |

Table III

| Parameter number | Parameter values | Remarks |
|---|---|---|
| 1 | 0·02102 | Variable |
| 2 | 0·01213 | Variable |
| 3 | 0·02735 | Variable |
| 4 | 0·00892 | Variable |
| 5 | 3·10000 | Variable |
| 6 | 0·60000 | Fixed |
| 7 | 3·10000 | Variable |
| 8 | 0·60000 | Fixed |
| 9 | 0·45700 | Fixed |
| 10 | 0·45100 | Fixed |

Table IV

| Parameter number | Parameter values Initial (iteration = 0) | Final (iteration = 5) |
|---|---|---|
| 1 | 0·01569 | 0·01682 |
| 2 | 0·00905 | 0·02062 |
| 3 | 0·02041 | 0·02188 |
| 4 | 0·00666 | 0·01516 |
| 5 | 2·40500 | 4·96000 |
| 6 | 0·62100 | 0·60000 |
| 7 | 2·24500 | 4·96000 |
| 8 | 0·56600 | 0·60000 |
| 9 | 0·45700 | 0·45700 |
| 10 | 0·45100 | 0·45100 |

## CONCLUSIONS

In this paper an attempt was made to identify the non-Darcy groundwater flow parameters of three different flow systems. The optimization of the coefficients for the first system was successfully achieved using an integral approach. However, in the second system the presence of 'noisy' data caused a number of problems. As a result, the solution strategy was directed towards an identification scheme which minimized a discharge error criterion within a bounded parametric domain in order to obtain physically plausible friction parameters. The optimization of the coefficients for the third system was also difficult due to the hybrid simulation of unsteady three-dimensional groundwater flow. In particular, some parameters influenced the solution far more than others. As a consequence, an interactive algorithm was developed whereby the validity of the parameters could be examined by the modeller at the end of each minimization step. A new set of coefficients was subsequently determined using Cauchy's steepest-descent method.

## REFERENCES

1. E. O. Frind and G. F. Pinder, 'Galerkin solution of the inverse problem for aquifer transmissivity', *Water Resources Res.*, **9** (5), 1397–1410 (1973).

2. D. Kleinecke, 'Use of linear programming for estimating geohydrologic parameters of groundwater basins', *Water Resources Res.*, **7** (2), 367–374 (1971).
3. K. Elango and H. S. Rao, 'Finite element description of flow fields in groundwater management models', in C. A. Brebbia, W. G. Gray and G. F. Pinder (eds), *Proc. Second Int. Conf. on Finite Elements in Water Resources*, Pentech Press, 1978. pp. 1.213–1.225.
4. V. Guvanasen and R. E. Volker, 'Identification of distributed parameters in groundwater basins', *J. Hydrol.*, **36**, 279–293 (1978).
5. A. Navarro, 'A modified optimization method of estimating aquifer parameters', *Water Resources Res.*, **13** (6), 935–939 (1977).
6. Y. Emsellem and G. de Marsily, 'An automatic solution for the inverse problem', *Water Resources Res.*, **7** (5), 1264–1283 (1971).
7. V. Vemuri, J. A. Dracup, R. C. Erdmann and N. Vemuri, 'Sensitivity analysis method of system identification and its potential in hydrologic research', *Water Resources Res.*, **5** (2), 341–349 (1969).
8. J. C. Bruch Jr., C. M. Lam and T. M. Simundich, 'Parameter identification in field problems', *Water Resources Res.*, **10** (1), 73–79 (1974).
9. D. A. Wismer, R. L. Perrine and Y. Y. Haimes, 'Modelling and identification of aquifer systems of high dimension', *Automatica*, **6**, 77–86 (1970).
10. Y. Bachmat and A. Dax, 'An iterative method for calibrating a multicell aquifer model', *Water Resources Res.*, **15** (2), 305–312 (1979).
11. R. L. Cooley, 'A method of estimating parameters and assessing reliability for models of steady state groundwater flow: 1, Theory and numerical properties', *Water Resources Res.*, **13** (2), 318–324 (1977).
12. A. Yziquel and J. C. Bernard, 'Automatic computing of a transmissivity distribution using only piezometric heads', in C. A. Brebbia, W. G. Gray and G. F. Pinder (eds), *Proc. Second Int. Conf. on Finite Elements in Water Resources*, Pentech Press, 1978, pp. 1.157–1.169.
13. L. Smith and R. A. Freeze, 'Stochastic analysis of steady state groundwater flow in a bounded domain: 2, Two-dimensional simulations', *Water Resources Res.*, **15** (6), 1543–1559 (1979).
14. W. W.-G. Yeh, 'Aquifer parameter identification', *Proc. ASCE, J. Hydraulics Div.*, **101** (HY9), 1197–1209 (1975).
15. S. P. Neuman, 'A statistical approach to the inverse problem of aquifer hydrology: 3, Improved solution method and added perspective', *Water Resources Res.*, **16** (2), 331–346 (1980).
16. J. P. Delhomme, 'Spatial variability and uncertainty in groundwater flow parameters: a geostatistical approach', *Water Resources Res.*, **15** (2), 269–280 (1979).
17. G. Gambolati and G. Volpi, 'Groundwater mapping in Venice by stochastic interpolators: 1 Theory', *Water Resources Res.*, **15** (2), 281–290 (1979).
18. G. J. Edgell, 'Unsteady flow to gravity wells', unpublished *Ph.D. Thesis*, University of Leeds, 1974.
19. D. C. Peters, 'Three-dimensional flow through a porous medium', unpublished *Ph.D. Thesis*, University of Leeds, 1974.
20. C. Kalliontzis, 'A finite element and non-Darcy groundwater flow study', unpublished *Ph.D. Thesis*, University of Leeds, 1981.
21. I. M. Goodwill and C. Kalliontzis, 'Three-dimensional non-Darcy flow analysis using a hybrid numerical model', *Appl. Math. Modelling*, **6**, 151–156 (1982).
22. J. A. McCorquodale, 'Variational approach to non-Darcy flow', *Proc. ASCE, J. Hydraulics Div.*, **96** (HY11), 2265–2278 (1970).
23. J. C. Nash, 'Compact numerical methods for computers: linear algebra and function minimisation', Adam Hilger, Bristol, 1979.
24. P. Basak, 'Steady non-Darcian seepage through embankments', *Proc. ASCE, J. Irrigation and Drainage Div.*, **102** (IR4), 435–443 (1976).